

Investigation of mercury (II) and copper (II) sorption in single and binary systems by alginate/polyethylenimine membranes

Yayuan Mo, Yue Zhang, Thierry Vincent, Catherine Faur, Eric Guibal

▶ **To cite this version:**

Yayuan Mo, Yue Zhang, Thierry Vincent, Catherine Faur, Eric Guibal. Investigation of mercury (II) and copper (II) sorption in single and binary systems by alginate/polyethylenimine membranes. Carbohydrate Polymers, 2021, 257, pp.117588. 10.1016/j.carbpol.2020.117588 . hal-03101254

HAL Id: hal-03101254

https://imt-mines-ales.hal.science/hal-03101254

Submitted on 1 Jun 2021

HAL is a multi-disciplinary open access archive for the deposit and dissemination of scientific research documents, whether they are published or not. The documents may come from teaching and research institutions in France or abroad, or from public or private research centers.

L'archive ouverte pluridisciplinaire **HAL**, est destinée au dépôt et à la diffusion de documents scientifiques de niveau recherche, publiés ou non, émanant des établissements d'enseignement et de recherche français ou étrangers, des laboratoires publics ou privés.

Investigation of mercury(II) and copper(II) sorption in single and binary systems by alginate/polyethylenimine membranes

Yayuan Mo [a,b,*], Yue Zhang [b], Thierry Vincent [b], Catherine Faur [c], Eric Guibal [b]

[a] College of Environment and Resources, Guangxi Normal University, Guilin, China
[b] PCH, IMT Mines Ales, Ales, France
[c] IEM, Institut Européen des Membranes, Univ Montpellier, CNRS, ENSCM, Montpellier, France

A B S T R A C T

This study investigates Hg(II) and Cu(II) sorption in single and binary systems by alginate/polyethylenimine membranes. Batch experiments are conducted to assess the metal sorption performance. FTIR and SEM-EDX analyses are used to identify metal binding mechanism. The sorption kinetics are better fitted by the pseudo-second-order-equation compared to the pseudo-first-order-equation. Three isotherms are compared for fitting the sorption in mono-component solutions and the Sips model gives the best simulation of experimental data. The competitive-Sips model fits well sorption data in Hg-Cu binary solutions and finds that the Cu uptake is drastically reduced by Hg competition. Copper(II) uptake remains negligible at low pH whereas it increases with pH up to 6 because of material deprotonation. Mercury(II) sorption behaves differently, it slightly changes from pH 1 (q_{eq}: 0.76 mmol g^{-1}) to pH 6 (q_{eq}: 0.84 mmol g^{-1}) due to chloro-anion formation. Therefore, playing with the pH allows separating Hg(II) from Cu(II).

Keywords:
Metal sorption
Alginate/polyethylenimine membrane
Copper
Mercury
Binary system
Recycling

1. Introduction

Industrialization and technological development expose our global environment and human beings to increasing levels of pollution. Pollution of water by heavy metals is one of the major threats (Korpayev, Kavaklı, Tilki, & Akkaş Kavaklı, 2018). Indeed, many industries (such as electroplating, smelting, printing and mining) are generating effluents containing various toxic metals which can be directly or indirectly discharged into the environment (Xu et al., 2018). International and regional regulations are thus becoming progressively more exigent for controlling the levels of metals released by industry, and for their concentration in drinking water. Several heavy metals have retained a specific attention because of their harmfulness to human health and ecosystems because of their highly toxicity, bioaccumulation and persistence, even at low concentrations (Saha et al., 2017). Lead(II), Cu (II), Cr(VI), Hg(II), and As(V) are emblematic examples of these hazardous elements (Niu, Deng, Yu, & Huang, 2010). These metals often exist in aqueous solution under the form of cations and anions (including oxyanions and chloro-anions) with different or even opposite properties (Kavakli, Barsbay, Tilki, Guven, & Kavakli, 2016; Lee et al., 2017). In some cases, institutional politics are also highly incentive for developing recycling processes for valorizing wastes, end-life equipment and for saving strategic resources (Gleick & Peter, 2000). All these reasons may explain the wide efforts made to develop new materials and new processes for metal recovery from aqueous systems and from solid wastes.

Many different processes may be used for recovering metal ions from aqueous solutions, depending on the composition and complexity of the solution. In particular, the choice of a process may depend on metal concentration (competitiveness), presence of ligands (metal speciation), flow rates of contaminated source (unit dimensioning), economic value of target metals and expected levels of decontamination. Solvent processes are meaningful for the recovery of valuable metals from acid and concentrated leachates and solutions (Kul & Oskay, 2015); precipitation techniques are useful for high flow rate effluents containing base metals (Fu & Wang, 2011); electrochemistry and membranes are more appropriate for smaller units of valuable metals (Diaz & Lister, 2018; Zhang et al., 2018). Sorption has been shown to be an economically feasible alternative for the removal of metals. From activated carbon, silica-based sorbents to synthetic chelating and ion-exchange resins, many sorbents have been designed for the recovery of metal ions (Faulconer, von Reitzenstein, & Mazyck, 2012; Oliva, De Pablo, Cortina, Cama, & Ayora, 2010; Prelot, Ayed, Marchandeau, & Zajac, 2014).

* Corresponding author at: College of Environment and Resources, Guangxi Normal University, Guilin, China.
E-mail addresses: moyayuan110@163.com (Y. Mo), Yue.Zhang@mines-ales.fr (Y. Zhang), Thierry.Vincent@mines-ales.fr (T. Vincent), Catherine.Faur@umontpellier.fr (C. Faur), Eric.Guibal@mines-ales.fr (E. Guibal).

However, for the last decades biosorption (based on the use of materials of biological origin bearing different functional groups) has also retained a great attention from research community (De Freitas, Da Silva, & Vieira, 2019; Mata, Blázquez, Ballester, González, & Muñoz, 2010).

Alginate is a non-toxic, abundant, cheap, renewable, biocompatible, and biodegradable biopolymer containing numerous free hydroxyl and carboxyl groups, which are available for metal ion binding (Pawar & Edgar, 2013). In addition, alginate may be easily used for designing new sorbents by chemical modification or by composite manufacturing (Zahra, Morteza, Mojgan, & Reza, 2018). Alginate-based materials may be conditioned under different shapes like hydrogels, beads and fibers by extrusion and ionotropic gelation; these conditionings have been successfully tested for improving metal sorption and/or facilitating their operative conditions (Dechojarassri et al., 2018; Fernando, Kim, Nah, & Jeon, 2019). According to the literature, improving the stability of alginate-based materials, achieving the facile solid-liquid separation and enhancing the recyclability and reusability are the critical challenges for the industrial-scale application of these materials (Li et al., 2013).

Recently, we described in a previous paper the design of alginate/polyethylenimine (alginate/PEI) membranes through the reaction of anionic carboxyl groups of negatively-charged alginate (in solution) with cationic amine groups of positively-charged PEI (Mo, Vincent, Faur, & Guibal, 2020). This interaction contributed to form a membrane gel, which is further stabilized by the crosslinking of primary amine groups (on PEI) with glutaraldehyde (GA). The fabrication procedure is easy to achieve without complicated operating conditions; the process does not require high energy consuming like freeze-drying process for elaborating highly porous materials. Remarkably, the as-prepared membrane with high permeability achieves outstanding natural drainage properties combined with high affinity for oxyanions Cr(VI) and Se(VI) (Mo et al., 2019, 2020). On the other side, it is still interesting to explore the applicability of this percolating membrane towards other forms of metal ions with different physicochemical properties (including reactivity with cations and chloride anions). In this study, two representative metals Cu(II) and Hg(II) are selected as models of pollutants to study the sorption performance of the alginate/PEI membrane in both mono-component and binary mixture. Copper ions are usually accompanied by mercury ions presented in effluents from a variety of industrial processes like chloro-alkali production, battery manufacturing and mining operations (Oliva, De Pablo, Cortina, Cama, & Ayora, 2011). Furthermore, Cu(II) is usually considered a borderline metal ions while Hg(II) is part of soft acids, according to Pearson's classification (or Hard and soft acids and bases (HSAB) theory) (Pearson, 1963). The comparison of their sorption properties in relation with metal speciation and HSAB properties of reactive groups is then of great interest for anticipating separation properties for metal recovery from real-like effluents containing several metal ions.

Theoretically, Cu(II) is a widespread heavy metal presented in stable cationic form in aqueous solution, which can be bound on amine groups through chelation and electrostatically attracted by negatively charged groups (Chen et al., 2010). On the opposite hand, Hg(II) easily forms chloro-anions (such as $HgCl_3^-$, $HgCl_4^{2-}$) in the presence of chloride ions; these anions can be easily attracted by protonated amine groups through electrostatic interaction, in addition to direct chelation of free mercury species onto carboxylate and non-protonated amine groups at higher pH values (Borreguero et al., 2018).

Thus, the main objectives of this work consist of:

(a) assessing the sorption and competitive sorption behaviors of the alginate/PEI membranes for the recovery of Cu(II) and Hg(II) in single and binary metal ion systems at different pH values, investigating uptake kinetics and sorption isotherms and evaluating metal desorption and sorbent recycling,

(b) exploring the binding mechanisms of the cationic Cu(II) ions and chloro-anionic Hg(II) ion binding onto the membranes using FTIR and SEM-EDX techniques,

(c) modeling sorption isotherms, uptake kinetics and clarifying the selectivity of alginate/PEI membrane for Hg(II) against Cu(II) through the plot of three-dimensional surfaces for sorption isotherms.

2. Materials and methods

2.1. Materials

Metal salts like mercury (II) chloride ($HgCl_2$, 99.5 %) and copper (II) nitrate ($Cu(NO_3)_2$, 99.5 %) were provided by Fluka (Switzerland). Sodium alginate powder (commercial reference: Protanal 200S) was purchased from FMC BioPolymer (Ayr, UK). The parameters (water content: 16.3 % (w/w), M/G ratio: 0.16/0.84, molar mass (M_w): 4.46×10^5 g mol^{-1}) of alginate biopolymer have been already characterized (Mo et al., 2019); the detailed procedures are reported in Supplementary Information (SI) section. Branched polyethylenimine (PEI, $M_w = 7.5 \times 10^5$ g mol^{-1}) and glutaraldehyde (GA) in 50 % (w/w) aqueous solution were obtained from Sigma–Aldrich (Saint-Louis, USA). All chemicals used in this study were of analytical grade and demineralized (DI) water was used in the whole study.

2.2. Synthesis of alginate/PEI membranes

The alginate/PEI membrane was fabricated in a facile pathway without implementing a complex drying process. The detailed procedure of membrane synthesis has already been documented (Mo et al., 2020); the main steps are reported in the SI section. Briefly, the membrane was formed by mixing alginate (4 %(w/w), 100 mL), DI (400 mL) and PEI (4 %(w/w), 35 mL) firstly to obtain a mixture; here, the pH of PEI was adjusted to pH 6.5 (for proper ionic interaction between protonated amine groups and carboxylate groups). After stirring, the mixture was rapidly poured into a rectangular container and maintained at room temperature for 24 h to structure the membrane. Afterward, the composite membrane was carefully washed three times and further cross-linked by immersion into 300 mL of DI water containing 2.5 mL of 50 % (w/w) GA. The composite membrane was maintained under slow shaking at 30 rpm for 24 h. Finally, the alginate/PEI membrane was washed-up with DI, before being air-dried at room temperature.

2.3. Characterization

FTIR spectra of materials were recorded between 4000 and 400 cm^{-1} using a FTIR Bruker VERTEX70 spectrometer (Bruker, Germany) though a Smart Orbit Accessory for Single-Reflection Attenuated Total Reflectance (ATR). The surface morphology and semi-quantitative elemental composition of materials were examined by scanning electron microscopy (SEM, Quanta FEG 200, Thermo Fisher Scientific, Mérignac, France) and energy dispersive X-ray analysis (EDX, Oxford Instruments France, Saclay, France).

2.4. Sorption experiments

All sorption experiments for mono- or bi-component solution were conducted at room temperature (20 ± 1 °C) by contacting a certain amount of as-prepared membrane discs with the metal-containing solution. The basic conditions of the experiments are reported in the caption of each figure while detailed sorption procedures and calculated methods are presented in the SI section.

2.5. Data analysis and test

Most of experiments were conducted in parallel and the results were

presented as the average values and standard deviation (SD) (Kaushal & Singh, 2017).

$$SD = \sqrt{\frac{1}{n-1}\sum_{i=1}^{n}(x_i - x_{ave})^2} \quad (1)$$

where x_{ave} is the average value of x and n is the number of experimental data points.

For the binary solution, the sorption preference of the membrane for Hg(II) or Cu(II) was determined by the selectivity coefficient ($SC_{Hg/Cu}$). The mathematical statement is (Ruthven, 1984):

$$SC_{Hg/Cu} = \frac{q_{eq,Hg} \times C_{eq,Cu}}{q_{eq,Cu} \times C_{eq,Hg}} \quad (2)$$

Here q_{eq} (mmol g^{-1}) and C_{eq} (mmol L^{-1}) represent the equilibrium sorption capacity and concentration of metal ions, respectively. If the value of $SC_{Hg/Cu}$ is larger than 1, Hg(II) ions are preferred; conversely, the Cu(II) ions would be preferred for $SC_{Hg/Cu} < 1$.

Moreover, in this study, the Chi-square test (χ^2) was used to estimate the degree of difference between the experimental data and the data obtained by calculating from the applied models. The mathematical equation can be written as (Naiya, Bhattacharya, & Das, 2009):

$$\chi^2 = \sum_{i=1}^{n}\frac{(q_{e,\exp} - q_{e,cal})^2}{q_{e,cal}} \quad (3)$$

where $q_{e,\ exp}$ (mmol g^{-1}) and $q_{e,\ cal}$ (mmol g^{-1}) are experimental and calculated sorption capacities, respectively; n is the number of experimental data points. The lower the χ^2 value, the most accurate is the fitting of experimental profile.

The Akaike information criterion (AIC) was also used for comparing the fitting of experimental profiles with models having different numbers of adjustable parameters (Falyouna, Eljamal, Maamoun, Tahara, & Sugihara, 2020). The lower the AIC value, the better the model fits the experimental profile.

2.6. Brief reminder on the characteristics of alginate/PEI membranes

Alginate/PEI membranes were formed by mixing alginate and PEI to obtain a structured hydrogel and subsequently improved stability by crosslinking between GA and amine groups of PEI. This double interaction (PEI/alginate, PEI/GA) makes it possible to produce porous membranes. Based on previous study (Mo et al., 2020), the density and porosity of the membrane are 0.048 ± 0.001 g cm^{-3} and 74 ± 1 %, respectively. In addition, the percolation properties were evaluated by placing the membrane (diameter: 24.5 mm; height: 6.5 ± 0.1 mm) in a column and imposing a constant height of the water column (corresponding to a pressure of 0.006 bar). Results showed that the water flux of the membrane is 13 ± 1 mL cm^{-2} min^{-1}, which means superficial flow velocities as high as 7.8 m h^{-1} can be reached under "natural draining conditions" (without pumping). This clearly demonstrates the highly percolating property of the membrane. The membranes can then be simply used by gravity percolation.

Moreover, the double crosslinking also gives the membrane a high stability: the mass loss of the membrane does not exceed 14 % under vigorous vibration conditions (i.e., 150 rpm); and the membrane is fully preserved after constant feeding of 3 days in a fixed-bed column.

The pH point of zero charge (pH_{PZC}) of membrane was found close to 6, which means the overall charge on membrane surface is positive in acidic solution (pH below 6). This helps the material electrostatically adsorbing negatively charged ions.

3. Results and discussion

3.1. Sorption performance study and modeling analysis

3.1.1. Determination of equilibrium time and uptake kinetics

In order to evaluate the global sorption performances of membranes, it is important to investigate the uptake kinetics for determining equilibrium time but also identifying the controlling steps in the process. Indeed, the sorption kinetics may be controlled by various diffusion pathways (including bulk, film and intraparticle diffusion), different reaction mechanisms (such as chelation and electrostatic interaction) or their simultaneous contributions (Crini, Peindy, Gimbert, & Robert, 2007; Quattrini et al., 2017). Deng et al. (Deng, Zhang, Wang, Zheng, & Wang, 2015) reported that polyacrylonitrile fibers have a fast sorption rate for Cu(II) and Hg(II) (without Cl^-) mainly due to the high collision possibility with chelate groups which was controlled by the diffusion and migration process of metal ions in the solution to the active site. Gavilan et al. (Gavilan et al., 2009) found that the time required for achieving the complete recovery of Hg(II) (in the presence of Cl^-) using thiocarbamoyl derivative of chitosan or for reaching the equilibrium was quite long (up to 3–4 days of contact) due to the resistance of intraparticle diffusion.

Fig. 1 shows the kinetic profiles for Cu(II) and Hg(II) sorption; the reaction time for equilibrium was set to 3 days. Under selected experimental conditions Cu(II) sorption by the membrane is faster than Hg(II): in the first 2 min, the recovery yields of Cu(II) and Hg(II) are 30 % (q_e = 0.39 mmol g^{-1}) and 6.3 % (q_e =0.08 mmol g^{-1}), respectively. For Cu(II) sorption, the equilibrium was reached within 24 h with a sorption capacity of 0.65 mmol g^{-1}. In the case of the Hg(II), the equilibrium was reached within 72 h, and the maximum sorption capacity reaches 0.93 mmol g^{-1}.

The pseudo-first order rate equation (PFORE) and the pseudo-second order rate equation (PSORE) were used to fit kinetic profiles (Reddad, Gerente, Andres, & Le Cloirec, 2002). The equations of PFORE and PSORE were initially designed for modeling the chemical reaction rates in homogeneous systems. The application of these equations was extended to the description of heterogeneous systems:

$$\text{PFORE}: \ ln(q_{eq,1} - q_t) = ln\ q_{eq,1} - k_1 t \quad (4)$$

$$\text{PSORE}: \frac{t}{q_t} = \frac{1}{k_2 \times q_{eq,2}^2} + \frac{t}{q_{eq,2}} \quad (5)$$

where $q_{eq,i}$ (mmol g^{-1}) and q_t (mmol g^{-1}) are the amounts of metal ions adsorbed onto membranes at equilibrium and at time t (i = 1 or 2), respectively, and k_1 (min^{-1}) and k_2 (g $mmol^{-1}$ min^{-1}) are the apparent

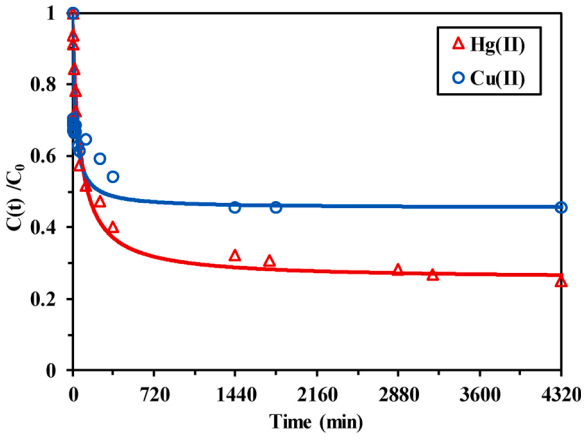


Fig. 1. Modeling of kinetic profiles (Metal concentration: 0.25 mmol L^{-1} of Cu (II) or Hg(II) single solution; Sorbent dosage = 0.2 g L^{-1}; initial pH = 5; T: 20 ± 1 °C; solid line: fit of kinetic profile with the PSORE).

rate constants of PFORE and PSORE models, respectively.

The parameters of the PFORE and PSORE models for sorption of metal ions onto the membrane are presented in Table 1; the determination coefficients (R^2) of Cu(II) and Hg(II) in PSORE model are both 0.999, indicating the PSORE equation fits better kinetic profiles than PFORE equation. This is also confirmed by: (a) the closer value of calculated equilibrium sorption capacity ($q_{eq,cal}$) to experimental equilibrium value ($q_{eq,exp}$) for PSORE than for PFORE, and (b) the superimposition of PSORE fitted curves with experimental points (Fig. 1). Moreover, the comparison of calculated rate constants of PSORE for Cu (II) (k_2: 0.066 g mmol^{-1} min^{-1}) and Hg(II) (k_2: 0.016 g mmol^{-1} min^{-1}) also confirmed that Cu(II) sorption by the membrane is faster than Hg (II). This is probably due to the fact that the molecular weight of the chloro-mercury complex is much higher than that of the Cu(II) cation, resulting in a lower diffusion rate under the same membrane sorption.

3.1.2. *Sorption isotherms for mono-/bi-component solutions*

The sorption isotherm plots the sorption capacity as a function of residual concentration at fixed temperature and pH value. The isotherm experiments in this study have been performed on both single and binary systems at pH 5. Analysis of isotherm data provides important information on the affinity of the sorbent for the solute and the saturation levels (maximum sorption capacity at monolayer coverage; for example, in the case of Langmuir model). Several classical models like Langmuir, Freundlich and Sips equations are frequently used for fitting the experimental profiles. Fig. 2 illustrates the sorption and competitive sorption behaviors for Hg(II) and Cu(II) in single and binary systems; relevant parameters are presented on Tables 2 and 3.

The Langmuir equation (Eq. 6) assumes that the sorption process takes place as a monolayer and occurs on the homogeneous surface of the sorbent (no interaction between sorbed species and equivalent binding energy for uptake of sorbate molecules onto reactive surface groups) (Lezcano et al., 2011). The Freundlich equation (Eq. 7) is used for describing multilayer sorption with non-uniform distribution of sorption heat and affinities on heterogeneous surface (Foo & Hameed, 2010). In addition, the Sips isotherm (Eq. 8) is a combination of Langmuir and Freundlich models: at low concentration, the Sips isotherm assumes the form of the Freundlich model, while at high concentration, it is similar to the Langmuir isotherm with finite saturation limit (Wang et al., 2018). Since the Sips equation includes a third-adjustable parameter, the mathematical fit is generally better than 2-adjustable parameters (such as Langmuir and Freundlich equation). The following equations were used:

$$\text{Langmuir}: q_{eq} = \frac{q_{m,L} \times b_L \times C_{eq}}{1 + b_L \times C_{eq}} \quad (6)$$

$$\text{Freundlich}: q_{eq} = k_F C_{eq}^{1/n_F} \quad (7)$$

$$\text{Sips}: q_{eq} = \frac{q_{m,S} \times b_S \times C_{eq}^{1/n_S}}{1 + b_S \times C_{eq}^{1/n_S}} \quad (8)$$

Table 1
Apparent kinetic parameters of the PFORE and PSORE models for the sorption of Hg(II) and Cu(II).

Model	Parameter	Hg(II)	Cu(II)
Experimental	$q_{eq,exp}$ (mmol g^{-1})	0.931	0.650
PFORE	$q_{eq,cal}$ (mmol g^{-1})	0.59 ± 0.16	0.31 ± 0.07
	$k_1 \times 10^3$ (min^{-1})	1.20 ± 0.09	3.50 ± 0.12
	R^2	0.928	0.984
	χ^2	1.66	0.04
PSORE	$q_{eq,cal}$ (mmol g^{-1})	0.93 ± 0.01	0.65 ± 0.02
	$k_2 \times 10^2$ (g mmol^{-1} min^{-1})	1.63 ± 0.38	6.63 ± 2.14
	R^2	0.999	0.999
	χ^2	1.46	0.33

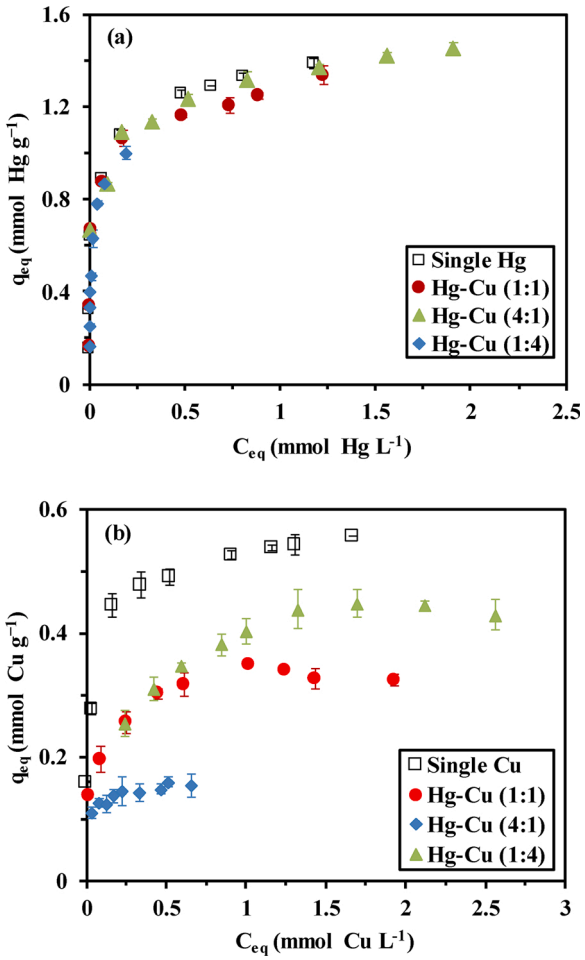


Fig. 2. Sorption and competitive sorption behaviors of (a) Hg(II) and (b) Cu(II) in single and binary systems (Sorbent dosage = 0.6 g L^{-1}; initial pH: 5; contact time =78 h; T = 20 ± 1 °C; Hg(II) or Cu(II) concentration: 0.1-2 mmol L^{-1} in single and Hg-Cu(1:1) solution; 0.1-2.8 mmol L^{-1} in Hg-Cu(4:1) and Hg-Cu (1:4). Note: Hg-Cu: the molar ratio of Hg(II) and Cu(II)).

Table 2
Sorption isotherms in mono-component solutions — Parameters for Langmuir, Freundlich and Sips equations.

Model	Parameter	Hg(II)	Cu(II)
Langmuir	$q_{max,exp}$ (mmol g^{-1})	1.39 ± 0.02	0.56 ± 0.003
	q_{mL} (mmol g^{-1})	1.27 ± 0.05	0.54 ± 0.002
	b_L (L mmol^{-1})	87.8 ± 26.1	40.8 ± 12.1
	R^2	0.94	0. 91
	χ^2	0.13	0.12
	AIC	−36	−54
Freundlich	k_F ((mmol g^{-1})/(L mmol^{-1})$^{1/n}$)	1.42 ± 0.06	0.53 ± 0.01
	n_F	4.81 ± 0.48	5.82 ± 0.65
	R^2	0.95	0.94
	χ^2	0.15	0.02
	AIC	−37	−58
Sips	q_{mS} (mmol g^{-1})	1.60 ± 0.14	0.66 ± 0.04
	b_S (L mmol^{-1})	5.37 ± 2.48	4.31 ± 1.34
	ns	1.97 ± 0.28	2.09 ± 0.22
	R^2	0.99	0.98
	χ^2	0.003	0.0002
	AIC	−46	−70

where C_{eq} (mmol L^{-1}) is the equilibrium concentration of metals; q_{eq} and $q_{m,j}$ (mmol g^{-1}) are the equilibrium and the maximum sorption capacities; bj is the affinity coefficient of Langmuir or Sips equation (j = L or S); k_F is the Freundlich constant, and n_F and n_S represent sorption

Table 3
Sorption isotherms in Hg-Cu binary system – Modeling constants for competitive Sips model.

Parameters	$q_{m,CS}$ (mmol g^{-1})	b_{Hg} (L mmol $^{-1}$)	b_{Cu} (L mmol $^{-1}$)	n_{Hg}	n_{Cu}	R^2	χ^2
Values	2.19 ± 0.16	1.94 ± 0.39	0.32 ± 0.04	2.57 ± 0.16	3.18 ± 0.41	0.97	0.005

intensity parameters for Freundlich and Sips equations, respectively.

As shown in Fig. 2, the sorption capacity of Hg(II) or Cu(II) in a single-component solution is characterized by a steep initial slope, followed by a saturation plateau. Interestingly, the saturation plateau for Hg(II) sorption reaches 1.39 mmol g^{-1}, while the saturated sorption capacity of Cu(II) is only 0.56 mmol g^{-1}; this means that the sorption capacity of membrane for Hg(II) is much higher than for Cu(II). Moreover, the three selected models fit well with the experimental data based on obtaining R^2 values (around 0.91−0.99) shown in Table 2. Thus, chi-square test (χ^2) and Akaike information criterion (AIC) were also applied to estimate the fit of sorption model. Based on the high R^2 (0.99 for Hg; 0.98 for Cu), low χ^2 values (0.003 for Hg; 0.0002 for Cu) and low AIC values (-46 for Hg; -70 for Cu), the best fit is obtained with the Sips equation. However, the Sips maximum sorption capacities for Hg(II) and Cu(II) in the single system reach up to 1.60 mmol g^{-1} and 0.66 mmol g^{-1}, respectively. Table S3 compares the maximum sorption capacities of alginate/PEI membrane with various similar sorbents reported in the literature. The as-prepared membrane in this study shows a relatively high sorption capacity for metals ions, especially for Hg(II). It is noteworthy that the alginate/PEI membrane has an important advantage related to its efficient Hg uptake in a very wide pH range (from 1 to 6). Moreover, the membrane shows a remarkable selectivity for Hg ions in the presence of copper (even in excess of competitor ion). This means that the membrane has a great potential in the recovery of Hg(II) from aqueous complex solutions, such as contaminated industrial effluents.

Since the isotherms for both Hg(II) and Cu(II) sorption onto the membrane obey the single-component Sips model, competitive Sips model was adopted to model the sorption data in binary system and quantify the competitive behavior of Hg(II)/Cu(II). The equation of competitive Sips model can be expressed as (Luna, Costa, da Costa, & Henriques, 2010):

$$\text{Sips (in binary system)} : q_{e,i} = \frac{q_{m,CS} \times b_i \times C_{e,i}^{1/n_i}}{1 + \sum_{j=1}^{2} b_j \times C_{e,j}^{1/n_j}} \quad (i \neq j) \tag{9}$$

where $q_{m,CS}$ (mmol g^{-1}) is the total maximum sorption capacity of Hg(II) and Cu(II) calculated from competitive Sips equation; b_i and b_j represent the affinity coefficient and n_i and n_j correspond to sorption intensity parameters. Based on this, the equations for Hg(II) and Cu(II) sorption in bi-component systems can be written as follows, respectively.

$$\text{For Hg(II)} : q_{e,Hg} = \frac{q_{m,CS} \times b_{Hg} \times C_{e,Hg}^{1/n_{Hg}}}{1 + b_{Hg} \times C_{e,Hg}^{1/n_{Hg}} + b_{Cu} \times C_{e,Cu}^{1/n_{Cu}}} \tag{10}$$

$$\text{For Cu(II)} : q_{e,Cu} = \frac{q_{m,CS} \times b_{Cu} \times C_{e,Cu}^{1/n_{Cu}}}{1 + b_{Hg} \times C_{e,Hg}^{1/n_{Hg}} + b_{Cu} \times C_{e,Cu}^{1/n_{Cu}}} \tag{11}$$

All experimental Hg(II) sorption isotherms in Hg–Cu binary solutions are almost superimposed to the mono-component Hg(II) sorption isotherm under selected experimental conditions (Fig. 2). For Cu(II) sorption, the sorption capacity obviously decreases in the presence of Hg (II) ions. In addition, the $SC_{Hg/Cu}$ in binary systems follows the order: Hg-Cu(1:4) (SC = 60.3) > Hg-Cu(1:1) (SC = 14.4) > Hg-Cu(4:1) (SC = 7.8); this means that the separation factor increases at elevated Cu content in mixture. This could be explained by the phenomenon that the increase of Cu ions has no significant effect on Hg sorption.

The constants ($q_{m,CS}$, b_i and n_i) in the competitive Sips model can be calculated by simultaneous nonlinear fitting of equations Eq. 10 and Eq. 11, using Origin software (OriginLab, v. 9.0, Northampton, MA, USA). The constants of the competitive Sips model for binary system are summarized on Table 3. The experimental data show a good compliance with the competitive Sips model in terms of R^2 (0.97) and χ^2 (0.005) values. Moreover, the cumulative sorption capacity of Hg(II) and Cu(II) is 2.19 mmol g^{-1}. To analyze sorption behaviors of Hg(II) and Cu(II) under binary sorption conditions, the modelled isotherms are also plotted in three-dimensional sorption surfaces using Origin software (Fig. 3). Obviously, increasing Hg(II) concentration leads to a dramatic fall in the sorption capacity of Cu(II). On the contrary, as the concentration of Cu(II) increases, Hg(II) sorption remains remarkably stable: these predicted results are consistent with those obtained from the binary sorption experiments. This is also consistent with the data collected from mono-component solutions.

Fig. S1 compares the sorption capacities for Cu(II) and Hg(II) in mono-component solutions with the cumulative sorption capacities of both ions (vs. cumulative residual concentration of both metal ions) for three different molar ratios between mercury and copper. In the presence of an excess of Hg(II) against Cu(II), Hg:Cu = 4:1, the cumulative sorption isotherm is superposed to the isotherm obtained with single-component Hg(II) solution. In equimolar binary solutions (Hg:Cu = 1:1), the saturation plateau is superposed to single-metal Hg(II) isotherm while the initial slope is decreased. On the opposite hand, the cumulative sorption capacity is strongly depreciated in the presence of an excess of copper (Hg:Cu = 1:4) and the saturation plateau is not reached in the concentration range investigated here. A higher concentration of Hg(II) would be necessary to achieve the saturation of the sorbent. Fig. S2 plots, for the three series, the evolution of the selectivity coefficient as a function of the equilibrium molar ration Hg(II)/Cu(II). Logically, the marked preference of the sorbent for mercury leads to high selectivity coefficients especially when copper is in excess compared with mercury (Ruthven, 1984). However, even in the presence of an excess of mercury, the $SC_{Hg/Cu}$ remains higher than 3, consistently with the greater affinity of alginate/PEI membranes for Hg (II).

3.2. *Sorption mechanism study*

3.2.1. *Characterization*

FTIR is one the most widely used technique for identifying the functional groups present at the surface of materials. The raw membrane and the membranes after reacting with Hg(II) and Cu(II) at pH 5.0 in both single and binary systems were analyzed by FTIR-ATR spectroscopy to highlight their sorption mechanisms.

The analysis mainly focuses on the most representative sections of spectra (Fig. 4). The full FTIR spectra and the assignments of the main peaks are presented in Fig. S3(a) and Table S1(a) (see SI Section), respectively. The main peaks of raw membrane are characterized at 3280 cm^{-1} (overlapped N–H and O–H stretching vibrations), 2927 cm^{-1} (C–H stretching), 1593 cm^{-1} (N–H bending and C=N vibration), 1406 cm^{-1} (COO^- symmetric stretching), 1316 cm^{-1} (C–N stretching vibration), 1089 cm^{-1} and 1030 cm^{-1} (C–O stretching vibration), and 947 cm^{-1} (C–H deformation) (Mo et al., 2020). After the sorption of metal ions (in both single and binary systems), several similar changes are observed:

(a) shift of the strong and wide peak at 3280 cm^{-1} due to the stretching vibration of amine and hydroxyl groups. It is noteworthy that the change of Cu(II)-loaded membrane is less marked compared with that of Hg(II)-loaded membrane (Fig. 4 and Table S1(a)). This means the involvement of amine and hydroxyl groups with Hg(II) is stronger in the case of mercury sorption,

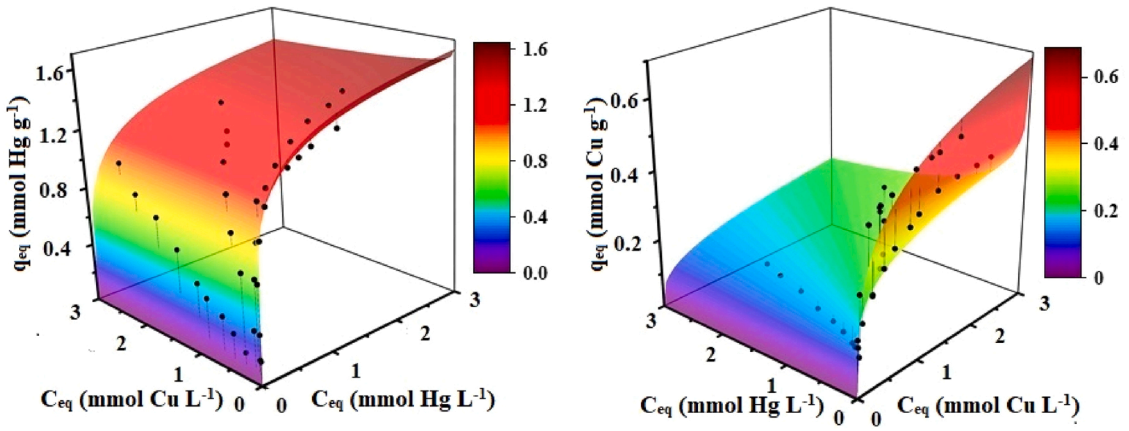


Fig. 3. Three-dimensional sorption surface plot showing competitive Sips model prediction and experimental data points.

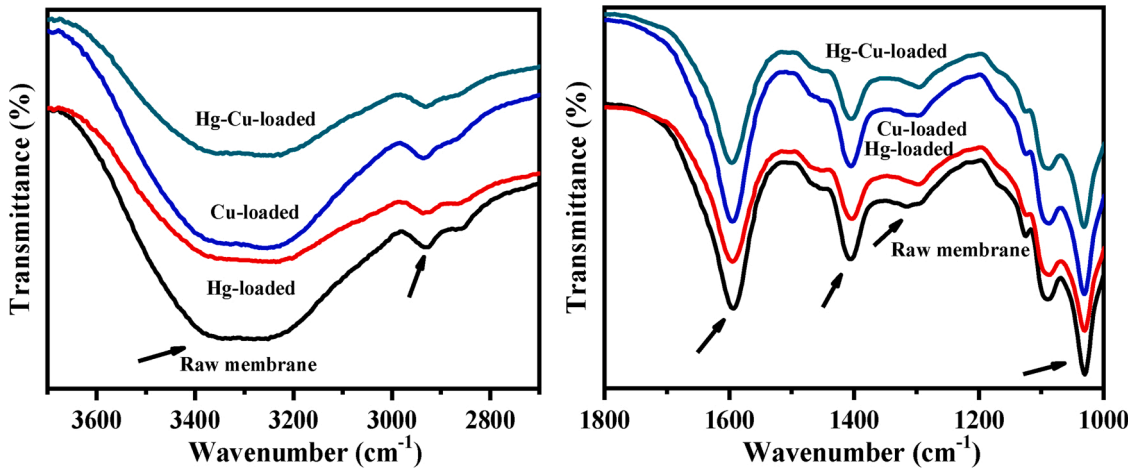


Fig. 4. FTIR spectra of membrane before and after Hg(II) and Cu(II) sorption in mono- or bi-component solution.

(b) shift of the peak at 2928 cm^{-1} (C–H stretching vibration); this means that C–H groups or their neighbor reactive groups are involved in metal binding process (Cimirro et al., 2020),
(c) shift and intensity decrease of the peak at 1316 cm^{-1} (C–N stretching vibration, resulting from the interaction between amine groups of PEI and aldehyde groups of GA) (Liu, Kuila, Kim, Ku, & Lee, 2013), which is associated with both metal binding,
(d) slightly decrease of the intensity of the peaks at 1406 cm^{-1} and 1030 cm^{-1}, which are assigned to COO^- symmetric stretching and C–O skeletal stretching vibrations of the carboxylate groups in alginate (Lawrie et al., 2007). This means carboxylate groups play a role in the sorption of Hg(II) and Cu(II).

In addition, the intensity of the peak at 1593 cm^{-1} slightly decreases after Hg(II) sorption and Hg-Cu sorption. This band may be associated with the vibrations of N–H (assigned to the primary amine groups of PEI) (Ouerghemmi et al., 2018) and C=N (due to the formation of Schiff bases generated by the reaction between PEI and GA) (Radi et al., 2016). The intensity decrease may be explained by the contribution of protonated amine groups in the specific binding of mercury species.

After the binary system sorption, the desorption of Hg(II)-Cu(II) loaded membranes using HCl, NaOH, thiourea and EDTA solution was studied. Their FTIR spectra and bands assignments were illustrated in Fig. S3(b) and Table S1(b) (see SI), respectively. The results showed that after desorption, the shapes of the spectra remain almost unchanged, except for the shifts of the peak at 3280 cm^{-1} (N–H and O–H or their overlaps stretching) and 1316 cm^{-1} (C–N stretching). This could be caused by the incomplete desorption of metals.

These analyses have thus shown that O–H, N–H, C–H, C–O and C–N identified on the membrane might participate in the process of Hg(II) and Cu(II) sorption, with a specific involvement of protonated amine groups in the case of mercury sorption.

In addition to FTIR analysis, SEM-EDX measurement is applied for analyzing the surface morphologies and semi-quantitative elemental compositions of the membranes before and after metal sorption (shown in Fig. 5). Apparently, Hg(II) and Cu(II) can be absorbed by the membranes in both single and binary systems. It is noteworthy that some white aggregates appear on the surface of the membrane after Hg(II) sorption (regardless of the single or binary system), while for Cu(II) not (Fig. 5). This difference may be related with the different sorption capacities and binding methods of Hg(II) and Cu(II). In addition, the EDX spectrum of raw membrane displays the presence of C and O elements (exceed 96 % in total, organic tracers) but also S, Na, Ca, Cl, Si, Mg and Al elements (residues of the extraction/shaping process of alginate). After Hg(II) sorption, many of these elements disappear (or their intensity dramatically decreases). The only elements significantly present are C, O, Hg and Cl; this reveals that mercury ions are strongly competitive against other metal cations (which may be exchanged with cations as Na, Ca, Si, Mg and Al elements). Simultaneously, the large increase in the content of chloride ions from 0.2 % to 2.7–3 % means that the binding of mercury onto the membrane must occur under the form of chloro-mercury species. The similar distribution of Hg and Cl elements (shown in Figs. S4–S7) also confirms that mercury ions are bound to the membrane simultaneously with chloride ions. On the opposite hand, the

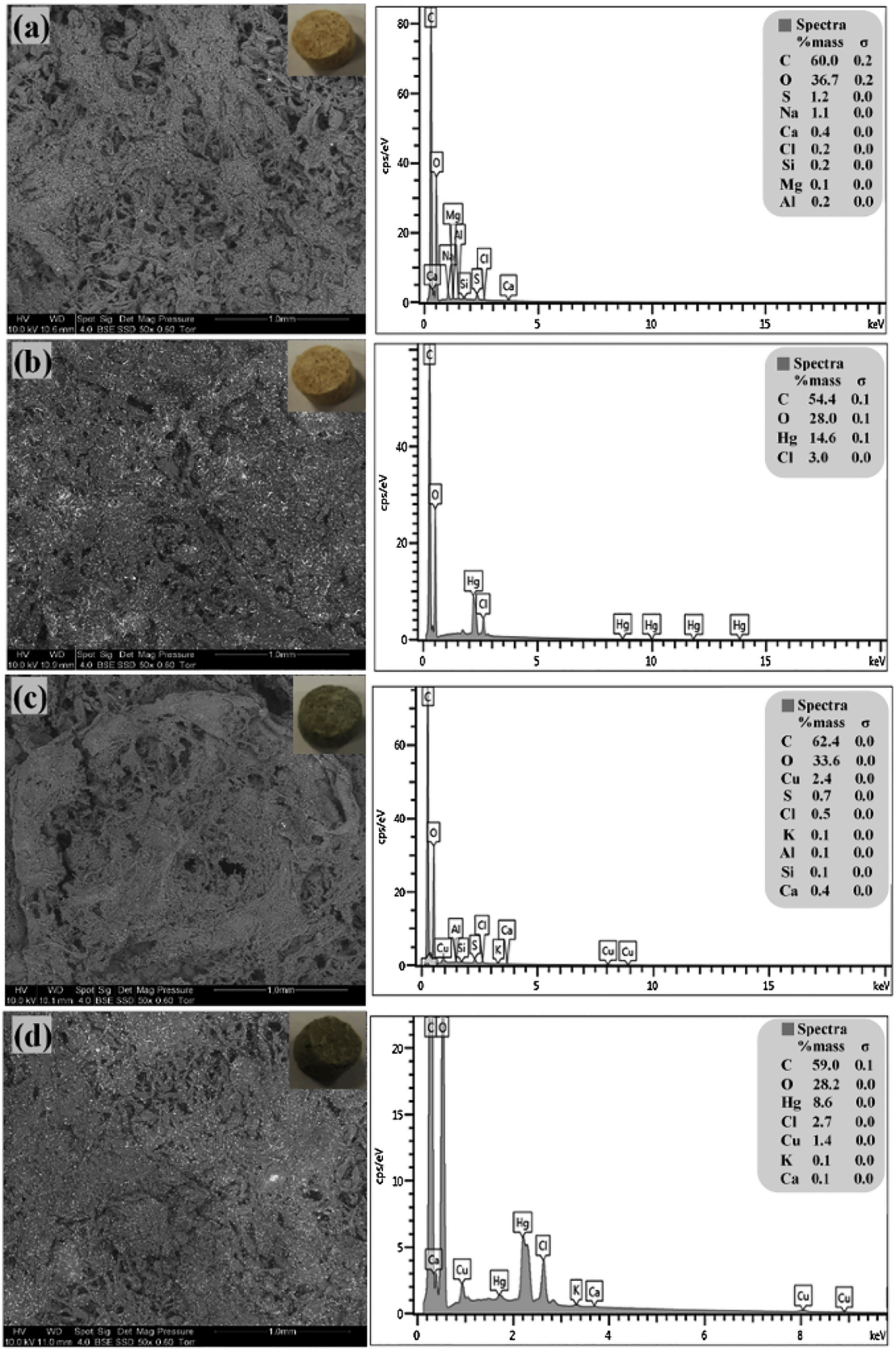


Fig. 5. SEM-EDX image of membranes (a) raw; (b) after Hg(II) sorption; (C) after Cu(II) sorption and (d) after Hg(II)-Cu(II) sorption.

elemental composition at the surface of the membrane is poorly affected by Cu(II) sorption. The unique exception concerns the disappearance of sodium ions. This may be explained by the ion exchange of Cu^{2+} with Na^{+} ions. The mapping of Cu element also shows the homogeneous distribution of Cu(II) binding on the membrane. In conclusion, the presences of mercury and copper peaks in the membrane confirm their successful loading onto the membrane. Copper ions are distributed densely and homogeneously on the surface of the sorbent, while Hg elements are found uniformly distributed on the surface of material even with a few aggregates.

3.2.2. *pH effect on sorption mechanism*

The pH of the solution is a critical parameter for sorption mechanism and performance since it may change the charge characteristics of the sorbent and the speciation of metal ions (Elwakeel & Al-Bogami, 2018). The pH effect was investigated in both single and binary systems to evaluate not only the impact of pH on the binding mechanism but also to study, playing with pH parameter, the possibility to use the sorption process in order to recover separately both metal ions from the effluent. To avoid precipitation phenomena which occurs above pH 6.5 for both Hg and Cu specifically (Hahne & Kroontje, 1973; Rahman & Islam, 2009), the initial pH (pH_0) variation was limited to 6. The results are presented in Fig. 6.

The pH has a significant impact on Cu(II) binding, while for Hg(II) recovery the change in sorption capacities is much less marked, for both mono- and bi-component solutions. Fig. S8a shows the sorption capacity vs. the initial pH of the solution. The membrane maintains a high affinity for Hg(II) ions under a wide pH range while for copper the sorption begins when initial pH is higher than 2. More representative of the equilibrium conditions, Fig. 6 shows the evolution of sorption capacities as a function of equilibrium pH (pH_{eq}). It is noteworthy that Hg(II) sorption capacity is higher than that of Cu(II), under selected experimental conditions. Fig. S8b reports the pH variation during metal binding. For pH_0 varying between 1 and 3, the pH remains unchanged, while above pH 3 the equilibrium pH tends to stabilize around 3.5–3.8, almost independently of the metal (including binary solutions). This pH buffering effect may result from the deprotonation of the functional groups like carboxylic groups and the release of protons.

Cu(II) is mostly present in solution under its cationic form in the pH range 1–6 (Wołowicz & Hubicki, 2012). For Cu sorption, it is obvious that at low pH (below pH 2) the sorption capacity is negligible (less than 0.006 mmol g^{-1}) in both single and binary systems. The high concentration of competitor ions H^{+} strongly limits the sorption capacity at low pH. The progressive increase of sorption capacity with the pH_0 up to 6 may be associated with the lower protonation of functional groups such as carboxylic groups (from alginate) at the surface of the membranes. The pK_a values of carboxylic groups in alginate are usually reported at 3.38 and 3.65 for mannuronic acid and guluronic acid, respectively (Haug, 1964). Thus, the deprotonation of the carboxylic groups ($COOH \rightarrow COO^{-} + H^{+}$) progressively increases with pH (especially for pH > 3.6); the surface charge becomes favorable to the sorption of Cu(II) cations (Nkoh, Yan, Xu, Shi, & Hong, 2020). This interpretation is consistent with the steep increase of Cu(II) sorption capacity in both single and binary systems when pH approaches pH 3.6 (Fig. 6). Similar conclusions were reported by Lim and Ge (Ge, Cui, Liao, & Li, 2017; Lim, Zheng, Zou, & Chen, 2008). On the other hand, many studies have reported PEI to be a specific ligand for various metal ions and the fact that Cu(II) can be bound on the donating nitrogen atoms of PEI by chelation in near-neutral solutions (Bessbousse, Rhlalou, Verchère, & Lebrun, 2008; Hudson & Matejka, 1989). PEI bears primary, secondary and tertiary amine groups (with pK_a values close to 4.5, 6.7 and 11.6, respectively (Demadis, Paspalaki, & Theodorou, 2011). Therefore, Cu(II) ions may also be chelated on primary amino groups at weak acidic or near-neutral pH (above pH 4.5).

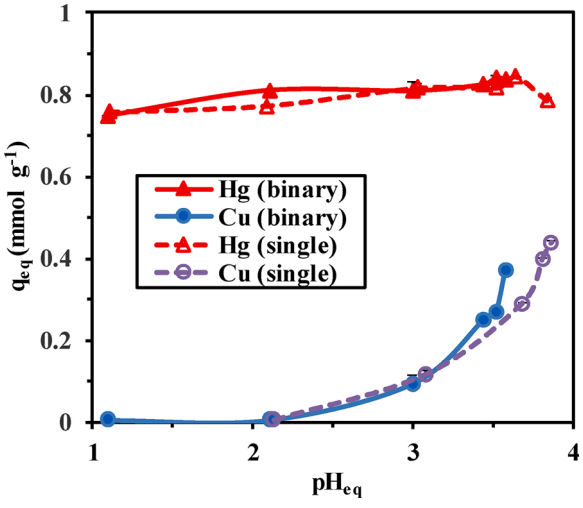


Fig. 6. Effect of pH on metal ions sorption in both single and binary systems (Metal concentration: 0.5 mmol L^{-1} of Cu(II) or Hg(II) single solution and 1.0 mmol L^{-1} of mixed [Hg(II):Pb(II) = 1:1] solution; Sorbent dosage = 0.5 g L^{-1}; contact time = 72 h; temperature = 20 ± 1 °C).

In the case of Hg(II), Fig. 6 and Fig. S8a show that the membrane can efficiently remove Hg(II) from both single and binary component systems within a wide pH_0 range (1–6) and that Hg(II) sorption capacities slightly increased from 0.76 mmol g^{-1} (at pH_0 1) to 0.84 mmol g^{-1} (around pH_0 5). This enhancement may be attributed to the specific property of Hg(II) to form chloro-complexes in the presence of Cl^{-} ions. As reported by Ranganathan (Ranganathan, 2003), different chloro-complexes can be formed in the presence of chloride anions including $HgCl_2$, $HgCl^{+}$, $HgCl_3^{-}$ and $HgCl_4^{2-}$. Fig. S9 shows the speciation of mercury (C_0: 0.5 mmol L^{-1}) as a function of pH, together with the corresponding concentration of chloride ion (calculated with Visual Minteq, (Gustafsson, 2013)). The predominant mercury species are $HgCl_2$, $HgCl_3^{-}$ and $HgCl_4^{2-}$ under selected conditions (pH range 0–4). It is noteworthy that the uncharged species $HgCl_2$ represent about 90–98 % in the pH range 2−4. The semi-quantitative EDX analysis of Hg (II)-loaded membranes (sorption at pH_0 5 and pH_{eq} 3.6) has shown, through the correlation in the distribution of Hg and Cl elements (mapping Fig. S5) that mercury is bound as a chloro-complex. However, the experimental results show, despite a slow increase with pH, that Hg (II) sorption capacity is almost unchanged at the different pH values, independently of the relative proportions of neutral ($HgCl_2$) and negatively-charged species ($HgCl_3^{-}$ and $HgCl_4^{2-}$). This probably means that the membrane may sorb these three species (including neutral $HgCl_2$), through different pathways: (a) electrostatic attraction of anionic chloro-complexes on protonated amine groups of PEI in acidic solutions (Ziebarth & Wang, 2014); and (b) by chelation of free or neutral mercury $HgCl_2$ species by primary amino groups of PEI and/or carboxylate groups of alginate at higher pH values. Sarkar et al. (Sarkar, Ansari, & Sen, 2016) investigated Hg(II) sorption by calcium alginate hydrogels; they pointed out that the uncharged $HgCl_2$ interacts with carboxylic acid groups by hydrogen bonding or van der Waal's forces. In the study of Hg(II) sorption by chemically modified polyaniline, Devi et al. (Devi, Kumar, Verma, & Sudersanan, 2006) also concluded that chloro-anionic mercury species can be bound on the protonated amine groups whereas neutral $HgCl_2$ species interact with unprotonated nitrogen. In highly acidic conditions (i.e., pH 1), the slight decrease in Hg (II) sorption capacity may be attributed to the competition effect of Cl^{-} (Guibal, Gavilan, Bunio, Vincent, & Trochimczuk, 2008).

The comparison of sorption behaviors in single and binary solutions (Fig. 6) shows that maximum Cu(II) sorption capacities decreases from 0.44 mmol g^{-1} in single-component solution to 0.37 mmol g^{-1} in binary solution whereas the presence of Cu(II) ions (at the same concentration) has no significant effect on Hg sorption capacity. The decrease in copper sorption capacity means that Hg(II) competes with Cu(II), and weaken

the ability of the membrane to bind Cu(II). The calculated $SC_{Hg/Cu}$ values (Table S2, see SI) are far higher than 1, which also confirms that the membrane has an obvious preference for Hg(II) than Cu(II). This preference for Hg(II) could be correlated with specific sorption mechanisms assumed from FTIR and EDX analysis and pH effect, but also with the physicochemical properties of the metals (such as ionic radii and ionic charge) (Dragan & Dinu, 2020) and HSAB principles (Pearson, 1963). Mercury is considered a soft acid, which binds preferentially to soft bases (bearing O- and N-groups), while copper is part of borderline acids (supposed to be less reactive with soft bases than mercury). Vieira et al. (Vieira, Guibal, Silva, & Beppu, 2007) obtained similar trends in the study of competitive sorption of Cu and Hg by chitosan membranes. They reported that the sorption capacity for Hg(II) was higher than for Cu(II) and suggested that this was probably due to the higher ionic radius of Hg(II) (i.e., 1.02 Å) compared with Cu(II) (i.e., 0.73 Å). In addition, the properties of the functional groups in the membrane are also playing a critical role in the sorption differences between Hg(II) and Cu(II). In the case of chitosan/zeolite cryogels, Humelnicu et al. (Humelnicu et al., 2020) found a correlation between the preference of the sorbent for a series of metal ions and their covalent index (i.e., χ^2/r). The covalent indexes of Hg(II) and Cu(II) are 4.08 and 2.64, respectively. The preference for Hg(II) over Cu(II) could thus be associated with a favored covalent binding of Hg(II) compared with Cu(II) because of the chemical structure of alginate/PEI membrane. The Gibbs free energy of formation (i.e., $\Delta G^{2+}_{f,M,\ aq}$) was used by Xu et al. (Xu, Xu, & Wang, 2017) for ranking the softness character of metal cations ($\Delta G^{2+}_{f,M,\ aq}$: 39.36 and 15.55 kJ mol^{-1} for Hg(II) and Cu(II)), respectively). Softness is coincidentally related to the tendency of a complex to form covalent bonds. However, these criteria may be modulated by the effect of metal speciation. In the case of mercury, the affinity of the soft base for chloride anions directly influences the speciation of the metal and its affinity for target reactive groups.

More interestingly, at low pH (pH 1–2) the membrane sorbent maintains a high affinity for Hg (0.76− 0.81 mmol g^{-1}), while the uptake for Cu is less than 0.006 mmol g^{-1}. This means that the membrane is superior acid-resistant and has an outstanding high selectivity for Hg over Cu in acidic environment. Fig. S6 shows that it is not possible correlating copper distribution with the mapping of chlorine. Indeed, a large increase occurs in the content of chloride ions after Hg binding onto the membrane while after Cu sorption it remains almost unchanged. This is another evidence that copper binding proceeds differently than mercury accumulation. In addition, Na(I) disappears completely after Cu(II) binding, which means a part of copper is bound on deprotonated carboxylic groups by ion exchange of Cu^{2+} with Na^+ ions. Obviously, in the case of binary solutions copper distribution is correlated to O mapping while Hg appears associated with chlorine (Fig. S7). It is noteworthy that Ca disappears after Hg(II) binding, while its relative fraction is not affected by copper binding when processing mono-component solutions. This trend is confirmed by the strong decrease in Ca content in the case of binary solutions (and predominance of mercury binding). This observation confirms that the mechanisms involved in metal sequestration are different for both metals. The absence of exchange between copper and calcium means that copper is probably bound by chelation on amine groups rather than free carboxylate groups.

3.2.3. Proposed sorption mechanism

In short, all the above analysis shows the possible mechanisms associated to the sorption of Hg(II) and Cu(II) ions onto membrane and their differences. The specific Hg(II) sorption mechanism consists of:

(a) electrostatic attraction of anionic chloro-complexes ($HgCl_3^-$ and $HgCl_4^{2-}$) on protonated amine groups of PEI;
(b) chelation of neutral mercury $HgCl_2$ species by primary amino groups of PEI and/or carboxylate groups of alginate;
(c) mercury elements are uniformly distributed on the surface of material even with a few aggregates.

The proposed mechanisms for Cu(II) sorption includes:

(a) ion-exchange with Na^+ ions and electrostatic attraction of copper cations on deprotonated carboxylate groups of alginate;
(b) chelation of Cu(II) by the donating nitrogen atoms of PEI (preferentially primary amines);
(c) copper ions are distributed densely and homogeneously on the surface of the membranes.

Considering that the main active sites for binding metals are amine groups (pKa: 4.5, 6.7 and 11.6) and carboxylic groups (pKa: 3.38 and 3.65) of the membranes, Fig. 7 presents the possible interaction mechanisms for Hg and Cu binding. As the pH study shows, the equilibrium pH tends to stabilize around 3.5−3.8. For $3.65 < pH_{eq} < 4.5$, carboxylic groups are deprotonated and primary amine groups begin to protonate. Therefore, deprotonated carboxylic groups ($-COO^-$), protonated amine groups ($-NH_3^+$) and free amino groups ($-NH_2$) are coexisted in aqueous solution. For $pH_{eq} < 3.65$, the carboxylic groups begin to protonate as (−COOH). Since the Cu(II) uptake is negligible at pH below 2, the carboxylic groups and amine groups are probable to be completely protonated in this case and poorly favorable for Cu(II) binding.

3.3. Metal desorption and sorbent recycling

Recycling ability of the sorbent is an important factor for assessing the cost-effectiveness of a sorption process in wastewater treatment. In this work, four different eluents (including HCl, NaOH, thiourea and EDTA) were tested for metal desorption from metal-loaded membranes (Fig. S10). It is found that 0.05 M HCl eluent exhibits poor efficiency for Hg(II) desorption contrary to Cu(II) elution. Copper sorption is highly sensitive to pH (with negligible sorption at pH 1); applying an acidic solution readily reverses the binding of copper cations. This is not the case for Hg(II) that can be readily bound on the membrane even in highly acidic solutions (due to the binding of chloro-anionic mercury species). The weak efficiency of HCl for Hg(II) release is thus consistent with previous findings. This also means that 0.05 M HCl solution can be used for selective release of Cu(II) from the sorbent when loaded with both Hg(II) and Cu(II). Other eluents (such as NaOH, thiourea and EDTA) show low desorption efficiencies for Hg(II) ions in the first cycle with metal recoveries of 3.2 %, 40.9 % and 42.1 %, followed by obvious increases after the first sorption-desorption process. At the third cycle, Hg recovery by the three eluents (i.e., NaOH, thiourea and EDTA) increases up to 31.3 %, 52.7 % and 90.3 % and the membranes still keep high affinity for Hg(II) (sorption capacity of 0.77 mmol g^{-1}, 0.72 mmol g^{-1} and 0.59 mmol g^{-1}). For the desorption of Cu(II) ions, at least for the first three sorption-desorption cycles, HCl and EDTA eluents show high desorption efficiency (higher than 91 %), with negligible effect on sorption performance. It is noteworthy that NaOH eluent greatly improves the sorption capacity of Cu(II) by the membrane at the following cycles. This may be caused by the presence of residual alkali that contributes to local micro-precipitation of copper. Despite abundant washing after NaOH elution step, the residual pH after metal binding is close to 6. Copper(II) ions cannot be released from the metal-loaded membrane by the NaOH solution. This means that the alkaline leaching offers a complementary selective step for the separation of Hg(II) from Cu(II).

In addition, after three cycles of sorption-desorption with the selected eluents (i.e., HCl, NaOH, thiourea and EDTA), the regenerated membranes maintain their shape and size. Notably, the structure of the membrane does not collapse. This also proves that the sorbent has a remarkable stability in strong acid or alkaline solutions.

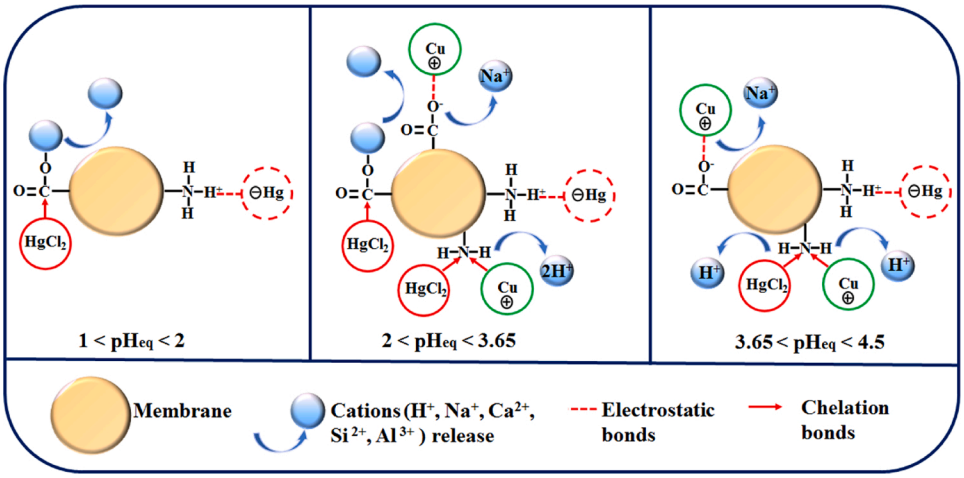


Fig. 7. Proposed mechanisms for Hg(II) and Cu(II) binding onto the membranes.

4. Conclusion

Alginate/PEI membranes are prepared and used for the sorption of Hg(II) and Cu(II) in mono-component solutions and binary mixtures. The FTIR analysis shows some shifts and changes in intensity for the characteristic bands of the amino groups, although the approximately overall shape of the spectra remains little affected by the sorption of metal ions.

The semi-quantitative EDX analysis confirms the binding of the two metal ions (alone or simultaneously bound for single- and binary solutions, respectively). Copper ions are distributed densely and homogeneously on the surface of the membrane, while Hg elements are uniformly distributed on the surface of the material (though few aggregates can be identified). It should be noted that the EDX reveals a correlation in the mapping of Hg and Cl elements: this is a confirmation that mercury binding occurs through the sorption of choro-complexes.

Sorption experiments reveal that the effect of the pH on metal binding strongly differs with the metal. Indeed, Cu(II) uptake by the membrane is negligible below pH_0 2 and increases with the pH_0 from 2 to 6 because of the lower protonation of the membrane. On the opposite hand, Hg(II) sorption capacity slightly changes from pH_0 1 (0.76 mmol g^{-1}) to pH_0 6 (0.84 mmol g^{-1}). This indicates the membrane can work over a wide pH range (1–6) for the effectively binding of Hg(II) and shows a remarkable high selectivity for this metal ion over Cu(II), in acidic conditions. The comparison of the binding kinetics (well fitted by the pseudo-second order equation) shows a higher sorption rate for copper (k_2, apparent rate constant: 0.066 g $mmol^{-1}$ min^{-1}) than for mercury (k_2: 0.016 g $mmol^{-1}$ min^{-1}). Isotherm study shows that the Sips equation allows a good simulation of the profile both in mono-component solution and binary mixture. The three-dimensional sorption surfaces (constructed by the competitive Sips equation) confirm that the increase of Hg(II) concentration led to a dramatic fall in the sorption capacity of Cu(II), while there is no obvious decrease in Hg(II) sorption as Cu(II) concentration increases. Sorption-desorption shows that the eluents HCl, thiourea and EDTA may involve copper release without significant impact on Cu(II) later sorption and the membranes maintain high affinity toward Hg(II) using NaOH, thiourea and EDTA as eluents, for at least three cycles. The membranes also demonstrate a remarkable stability in the process of desorption while using strong acid or alkaline solutions (porous structure, as shown by SEM observations, and functional groups, as confirmed by the stability of sorption performance).

CRediT authorship contribution statement

Yayuan Mo: Writing - original draft, Data curation. **Yue Zhang:** Investigation. **Thierry Vincent:** Methodology. **Catherine Faur:** Supervision, Writing - review & editing. **Eric Guibal:** Conceptualization, Supervision, Writing - review & editing.

Acknowledgments

Y. Mo acknowledges the China Scholarship Council (CSC, Grant N° 201708450080) for providing PhD fellowship. Y. Zhang acknowledges the China Scholarship Council (CSC, Grant N° 201906660008) for providing PhD fellowship. Authors thank Jean-Claude Roux (IMT Mines Alès, C2MA) for his technical support for SEM and SEM-EDX analyses.

References

Bessbousse, H., Rhlalou, T., Verchère, J.-F., & Lebrun, L. (2008). Removal of heavy metal ions from aqueous solutions by filtration with a novel complexing membrane containing poly(ethyleneimine) in a poly(vinyl alcohol) matrix. *Journal of Membrane Science, 307*(2), 249–259.

Borreguero, A. M., Leura, A., Rodríguez, J. F., Vaselli, O., Nisi, B., Higueras, P. L., et al. (2018). Modelling the mercury removal from polluted waters by using TOMAC microcapsules considering the metal speciation. *Chemical Engineering Journal, 341*, 308–316.

Chen, Y., Pan, B., Li, H., Zhang, W., Lv, L., & Wu, J. (2010). Selective removal of Cu(II) ions by using cation-exchange resin-supported polyethyleneimine (PEI) nanoclusters. *Environmental Science & Technology, 44*(9), 3508–3513.

Cimirro, N. F., Lima, E. C., Cunha, M. R., Dias, S. L., Thue, P. S., Mazzocato, A. C., et al. (2020). Removal of pharmaceutical compounds from aqueous solution by novel activated carbon synthesized from lovegrass (*Poaceae*). *Environmental Science and Pollution Research*, 1–13.

Crini, G., Peindy, H. N., Gimbert, F., & Robert, C. (2007). Removal of CI Basic Green 4 (Malachite Green) from aqueous solutions by adsorption using cyclodextrin-based adsorbent: Kinetic and equilibrium studies. *Separation and Purification Technology, 53*(1), 97–110.

De Freitas, G. R., Da Silva, M. G. C., & Vieira, M. G. A. (2019). Biosorption technology for removal of toxic metals: A review of commercial biosorbents and patents. *Environmental Science and Pollution Research*, 1–22.

Dechojarassri, D., Omote, S., Nishida, K., Omura, T., Yamaguchi, H., Furuike, T., et al. (2018). Preparation of alginate fibers coagulated by calcium chloride or sulfuric acid: Application to the adsorption of Sr^{2+}. *Journal of Hazardous Materials, 355*, 154–161.

Demadis, K. D., Paspalaki, M., & Theodorou, J. (2011). Controlled release of bis (phosphonate) pharmaceuticals from cationic biodegradable polymeric matrices. *Industrial & Engineering Chemistry Research, 50*(9), 5873–5876.

Deng, S., Zhang, G., Wang, X., Zheng, T., & Wang, P. (2015). Preparation and performance of polyacrylonitrile fiber functionalized with iminodiacetic acid under microwave irradiation for adsorption of Cu(II) and Hg(II). *Chemical Engineering Journal, 276*, 349–357.

Devi, P. R., Kumar, S., Verma, R., & Sudersanan, M. (2006). Sorption of mercury on chemically synthesized polyaniline. *Journal of Radioanalytical and Nuclear Chemistry, 269*(1), 217–222.

Diaz, L. A., & Lister, T. E. (2018). Economic evaluation of an electrochemical process for the recovery of metals from electronic waste. *Waste Management, 74*, 384–392.

Dragan, E. S., & Dinu, M. V. (2020). Advances in porous chitosan-based composite hydrogels: Synthesis and applications. *Reactive & Functional Polymers, 146*, Article 104372.

Elwakeel, K. Z., & Al-Bogami, A. S. (2018). Influence of Mo(VI) immobilization and temperature on As(V) sorption onto magnetic separable poly p-phenylenediamine-thiourea-formaldehyde polymer. *Journal of Hazardous Materials, 342*, 335–346.

Falyouna, O., Eljamal, O., Maamoun, I., Tahara, A., & Sugihara, Y. (2020). Magnetic zeolite synthesis for efficient removal of cesium in a lab-scale continuous treatment system. *Journal of Colloid and Interface Science*.

Faulconer, E. K., von Reitzenstein, N. V. H., & Mazyck, D. W. (2012). Optimization of magnetic powdered activated carbon for aqueous Hg(II) removal and magnetic recovery. *Journal of Hazardous Materials, 199*, 9–14.

Fernando, I. S., Kim, D., Nah, J.-W., & Jeon, Y.-J. (2019). Advances in functionalizing fucoidans and alginates (bio) polymers by structural modifications: A review. *Chemical Engineering Journal, 355*, 33–48.

Foo, K. Y., & Hameed, B. H. (2010). Insights into the modeling of adsorption isotherm systems. *Chemical Engineering Journal, 156*(1), 2–10.

Fu, F., & Wang, Q. (2011). Removal of heavy metal ions from wastewaters: A review. *Journal of Environmental Management, 92*(3), 407–418.

Gavilan, K. C., Pestov, A., Garcia, H. M., Yatluk, Y., Roussy, J., & Guibal, E. (2009). Mercury sorption on a thiocarbamoyl derivative of chitosan. *Journal of Hazardous Materials, 165*(1–3), 415–426.

Ge, Y., Cui, X., Liao, C., & Li, Z. (2017). Facile fabrication of green geopolymer/alginate hybrid spheres for efficient removal of Cu(II) in water: Batch and column studies. *Chemical Engineering Journal, 311*, 126–134.

Gleick, & Peter, H. (2000). A look at twenty-first century water resources development. *Water International, 25*(1), 127–138.

Guibal, E., Gavilan, K. C., Bunio, P., Vincent, T., & Trochimczuk, A. (2008). Cyphos IL 101 (tetradecyl (trihexyl) phosphonium chloride) immobilized in biopolymer capsules for Hg(II) recovery from HCl solutions. *Separation Science and Technology, 43*(9–10), 2406–2433.

Gustafsson, J. (2013). *Visual MINTEQ. Version 3.1. Division of land and water resources*. Stockholm, Sweden: Royal Institute of Technology. http://www2.lwr.kth.se/English /Oursoftware/vminteq/download.html.

Hahne, H., & Kroontje, W. (1973). Significance of pH and chloride concentration on behavior of heavy metal pollutants: Mercury(II), cadmium(II), zinc(II), and lead(II). *Journal of Environmental Quality, 2*(4), 444–450.

Haug, A. (1964). Composition and properties of alginates. *Plant Physiology, 105*(1), 205–213.

Hudson, M. J., & Matejka, Z. (1989). Extraction of copper by selective ion exchangers with pendent ethyleneimine groups—Investigation of active states. *Separation Science and Technology, 24*(15), 1417–1426.

Humelnicu, D., Lazar, M. M., Ignat, M., Dinu, I. A., Dragan, E. S., & Dinu, M. V. (2020). Removal of heavy metal ions from multi-component aqueous solutions by eco-friendly and low-cost composite sorbents with anisotropic pores. *Journal of Hazardous Materials, 381*, Article 120980.

Kaushal, A., & Singh, S. (2017). Critical analysis of adsorption data statistically. *Applied Water Science, 7*(6), 3191–3196.

Kavakli, C., Barsbay, M., Tilki, S., Guven, O., & Kavakli, P. A. (2016). Activation of Polyethylene/Polypropylene nonwoven fabric by radiation-induced grafting for the removal of Cr(VI) from aqueous solutions. *Water, Air, and Soil Pollution, 227*(12), 473.

Korpayev, S., Kavaklı, C., Tilki, S., & Akkaş Kavaklı, P. (2018). Novel cotton fabric adsorbent for efficient As(V) adsorption. *Environmental Science and Pollution Research, 25*, 34610–34622.

Kul, M., & Oskay, K. O. (2015). Separation and recovery of valuable metals from real mix electroplating wastewater by solvent extraction. *Hydrometallurgy, 155*, 153–160.

Lawrie, G., Keen, I., Drew, B., Chandler-Temple, A., Rintoul, L., Fredericks, P., et al. (2007). Interactions between alginate and chitosan biopolymers characterized using FTIR and XPS. *Biomacromolecules, 8*(8), 2533–2541.

Lee, C. G., Alvarez, P. J. J., Nam, A., Park, S. J., Do, T., Choi, U. S., et al. (2017). Arsenic (V) removal using an amine-doped acrylic ion exchange fiber: Kinetic, equilibrium, and regeneration studies. *Journal of Hazardous Materials, 325*, 223–229.

Lezcano, J., González, F., Ballester, A., Blázquez, M., Muñoz, J., & García-Balboa, C. (2011). Sorption and desorption of Cd, Cu and Pb using biomass from an eutrophized habitat in monometallic and bimetallic systems. *Journal of Environmental Management, 92*(10), 2666–2674.

Li, X., Qi, Y., Li, Y., Zhang, Y., He, X., & Wang, Y. (2013). Novel magnetic beads based on sodium alginate gel crosslinked by zirconium(IV) and their effective removal for Pb^{2+} in aqueous solutions by using a batch and continuous systems. *Bioresource Technology, 142*, 611–619.

Lim, S.-F., Zheng, Y.-M., Zou, S.-W., & Chen, J. P. (2008). Characterization of copper adsorption onto an alginate encapsulated magnetic sorbent by a combined FT-IR, XPS, and mathematical modeling study. *Environmental Science & Technology, 42*(7), 2551–2556.

Liu, H., Kuila, T., Kim, N. H., Ku, B.-C., & Lee, J. H. (2013). In situ synthesis of the reduced graphene oxide–polyethyleneimine composite and its gas barrier properties. *Journal of Materials Chemistry A, 1*(11), 3739–3746.

Luna, A. S., Costa, A. L., da Costa, A. C. A., & Henriques, C. A. (2010). Competitive biosorption of cadmium(II) and zinc(II) ions from binary systems by *Sargassum filipendula*. *Bioresource Technology, 101*(14), 5104–5111.

Mata, Y., Blázquez, M., Ballester, A., González, F., & Muñoz, J. (2010). Studies on sorption, desorption, regeneration and reuse of sugar-beet pectin gels for heavy metal removal. *Journal of Hazardous Materials, 178*(1–3), 243–248.

Mo, Y., Wang, S., Vincent, T., Desbrieres, J., Faur, C., & Guibal, E. (2019). New highly-percolating alginate-PEI membranes for efficient recovery of chromium from aqueous solutions. *Carbohydrate Polymers, 225*, Article 115177.

Mo, Y., Vincent, T., Faur, C., & Guibal, E. (2020). Se(VI) sorption from aqueous solution using alginate/polyethylenimine membranes: Sorption performance and mechanism. *International Journal of Biological Macromolecules, 147*, 832–843.

Naiya, T. K., Bhattacharya, A. K., & Das, S. K. (2009). Adsorption of Cd(II) and Pb(II) from aqueous solutions on activated alumina. *Journal of Colloid and Interface Science, 333*(1), 14–26.

Niu, L., Deng, S., Yu, G., & Huang, J. (2010). Efficient removal of Cu(II), Pb(II), Cr(VI) and As(V) from aqueous solution using an aminated resin prepared by surface-initiated atom transfer radical polymerization. *Chemical Engineering Journal, 165*(3), 751–757.

Nkoh, J. N., Yan, J., Xu, R.-K., Shi, R.-y., & Hong, Z.-n. (2020). The mechanism for inhibiting acidification of variable charge soils by adhered Pseudomonas fluorescens. *Environmental Pollution, 260*, Article 114049.

Oliva, J., De Pablo, J., Cortina, J.-L., Cama, J., & Ayora, C. (2010). The use of Apatite IITM to remove divalent metal ions zinc(II), lead(II), manganese(II) and iron(II) from water in passive treatment systems: Column experiments. *Journal of Hazardous Materials, 184*(1–3), 364–374.

Oliva, J., De Pablo, J., Cortina, J.-L., Cama, J., & Ayora, C. (2011). Removal of cadmium, copper, nickel, cobalt and mercury from water by Apatite IITM: Column experiments. *Journal of Hazardous Materials, 194*, 312–323.

Ouerghemmi, S., Dimassi, S., Tabary, N., Leclercq, L., Degoutin, S., Chai, F., et al. (2018). Synthesis and characterization of polyampholytic aryl-sulfonated chitosans and their in vitro anticoagulant activity. *Carbohydrate Polymers, 196*, 8–17.

Pawar, S. N., & Edgar, K. J. (2013). Alginate esters via chemoselective carboxyl group modification. *Carbohydrate Polymers, 98*(2), 1288–1296.

Pearson, R. G. (1963). Hard and soft acids and bases. *Journal of the American Chemical Society, 85*(22), 3533–3539.

Prelot, B., Ayed, I., Marchandeau, F., & Zajac, J. (2014). On the real performance of cation exchange resins in wastewater treatment under conditions of cation competition: The case of heavy metal pollution. *Environmental Science and Pollution Research, 21*(15), 9334–9343.

Quattrini, F., Galceran, J., David, C., Puy, J., Alberti, G., & Rey-Castro, C. (2017). Dynamics of trace metal sorption by an ion-exchange chelating resin described by a mixed intraparticle/film diffusion transport model. The Cd/Chelex case. *Chemical Engineering Journal, 317*, 810–820.

Radi, S., Toubi, Y., El-Massaoudi, M., Bacquet, M., Degoutin, S., & Mabkhot, Y. N. (2016). Efficient extraction of heavy metals from aqueous solution by novel hybrid material based on silica particles bearing new Schiff base receptor. *Journal of Molecular Liquids, 223*, 112–118.

Rahman, M. S., & Islam, M. R. (2009). Effects of pH on isotherms modeling for Cu(II) ions adsorption using maple wood sawdust. *Chemical Engineering Journal, 149*(1–3), 273–280.

Ranganathan, K. (2003). Adsorption of Hg(II) ions from aqueous chloride solutions using powdered activated carbons. *Carbon, 41*(5), 1087–1092.

Reddad, Z., Gerente, C., Andres, Y., & Le Cloirec, P. (2002). Adsorption of several metal ions onto a low-cost biosorbent: Kinetic and equilibrium studies. *Environmental Science & Technology, 36*(9), 2067–2073.

Ruthven, D. M. (1984). *Principles of adsorption and adsorption processes*. John Wiley & Sons.

Saha, N., Rahman, M. S., Ahmed, M. B., Zhou, J. L., Ngo, H. H., & Guo, W. (2017). Industrial metal pollution in water and probabilistic assessment of human health risk. *Journal of Environmental Management, 185*, 70–78.

Sarkar, K., Ansari, Z., & Sen, K. (2016). Detoxification of Hg(II) from aqueous and enzyme media: Pristine vs. tailored calcium alginate hydrogels. *International Journal of Biological Macromolecules, 91*, 165–173.

Vieira, R. S., Guibal, E., Silva, E. A., & Beppu, M. M. (2007). Adsorption and desorption of binary mixtures of copper and mercury ions on natural and crosslinked chitosan membranes. *Adsorption, 13*(5–6), 603–611.

Wang, W., Zhao, Y., Bai, H., Zhang, T., Ibarra-Galvan, V., & Song, S. (2018). Methylene blue removal from water using the hydrogel beads of poly(vinyl alcohol)-sodium alginate-chitosan-montmorillonite. *Carbohydrate Polymers, 198*, 518–528.

Wołowicz, A., & Hubicki, Z. (2012). The use of the chelating resin of a new generation Lewatit MonoPlus TP-220 with the bis-picolylamine functional groups in the removal of selected metal ions from acidic solutions. *Chemical Engineering Journal, 197*, 493–508.

Xu, H., Xu, D. C., & Wang, Y. (2017). Natural indices for the chemical hardness/softness of metal cations and ligands. *ACS Omega, 2*(10), 7185–7193.

Xu, L., Xu, X., Cao, G., Liu, S., Duan, Z., Song, S., et al. (2018). Optimization and assessment of Fe-electrocoagulation for the removal of potentially toxic metals from real smelting wastewater. *Journal of Environmental Management, 218*(15), 129–138.

Zahra, E., Morteza, E., Mojgan, Z., & Reza, F. (2018). Controlling alginate oxidation conditions for making alginate-gelatin hydrogels. *Carbohydrate Polymers, 198*, 509–517.

Zhang, L., Zha, X., Zhang, G., Gu, J., Zhang, W., Huang, Y., et al. (2018). Designing a reductive hybrid membrane to selectively capture noble metallic ions during oil/water emulsion separation with further function enhancement. *Journal of Materials Chemistry A, 6*(22), 10217–10225.

Ziebarth, J. D., & Wang, Y. (2014). Understanding the protonation behavior of linear polyethylenimine in solutions through Monte Carlo simulations. *Biomacromolecules, 11*(1), 28–29.